

## Two-Stage, High Power X-Band Amplifier Experiment \*

E. Kuang, T. J. Davis, J. D. Ivers, G. S. Kerslick, J. A. Nation and L. Schächter  
 Laboratory of Plasma Studies and School of Electrical Engineering  
 Cornell University, Ithaca, NY 14853, USA

### Abstract

At output powers in excess of 100 MW we have noted the development of sidebands in many TWT structures. To address this problem an experiment using a narrow bandwidth, two-stage TWT is in progress. The TWT amplifier consists of a dielectric ( $\epsilon = 5$ ) slow-wave structure, a 30 dB sever section and a 8.8–9.0 GHz passband periodic, metallic structure. The electron beam used in this experiment is a 950 kV, 1 kA, 50 ns pencil beam propagating along an applied axial field of 9 kG. The dielectric first stage has a maximum gain of 30 dB measured at 8.87 GHz, with output powers of up to 50 MW in the  $TM_{01}$  mode. In these experiments the dielectric amplifier output power is about 3–5 MW and the output power of the complete two-stage device is  $\sim 160$  MW at the input frequency. The sidebands detected in earlier experiments have been eliminated. We also report measurements of the energy spread of the electron beam resulting from the amplification process. These experimental results are compared with MAGIC code simulations and analytic work we have carried out on such devices.

### I. INTRODUCTION

Earlier experiments [1] using two-stage ripple wall TWTs with  $\sim 1.8$  GHz bandwidths have achieved output powers in excess of 400 MW at  $\sim 9$  GHz. However at these levels up to 50% of the output power is emitted in asymmetric sidebands. Analytic work [2] has suggested that this process is due to finite length effects and reflections from the transition regions in the slow wave structures. To address this problem we have designed several low group velocity, narrow band structures (NBS) to effectively transit time isolate the input from the output. In addition since the inner diameter of these slow wave structures is beyond cutoff we achieve significant attenuation of any reflected signal from the output. For the forward amplifying wave the attenuation is unimportant because the electron beam couples successive cavities of the amplifier.

The interaction in the narrow band structure has been studied both analytically and with the particle-in-cell code MAGIC. As a result of the interaction process the energy spread of *individual* electrons can be as high as 60% of the initial beam energy, while the *average* energy of the beam is reduced by less than 10%. The analytical results indicate that a gain of 5–7 dB/cm can be expected compared to 1–2 dB/cm in the broad passband structure. This results from the high shunt impedance of

the narrow bandwidth structure. In this work the shunt impedance is defined by the relation

$$Z_{sh} = \frac{E_z^2(r = R_b)\pi r_i^2}{2P}$$

where  $E_z(r = R_b)$  is the longitudinal electric field at the beam location,  $r_i$  is the inner radius of the structure, and  $P$  is the total power which flows in the system (both quantities are calculated in the absence of the beam). The high shunt impedance of the narrow bandwidth amplifiers leads to high values of electric field in the structure. Calculations and simulation results show that for output powers of 200 MW the electric field on the wall will be  $\sim 200$  MV/m.

### II. EXPERIMENT

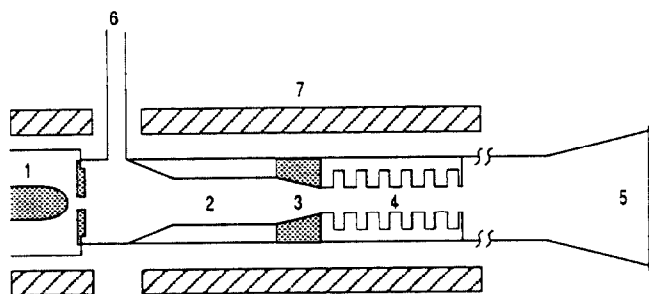


Fig 1. Schematic of the two-stage narrow band amplifier. (1) E-beam diode, (2) dielectric slow wave structure, (3) silicon carbide sever, (4) narrow band structure, (5) output horn, (6) input waveguide, (7) magnetic field coil.

The dielectric first stage of the amplifier (fig. 1) preamplifies the 20–50 kW magnetron input by  $\sim 20$  dB. A silicon carbide sever is used to attenuate by 30 dB the rf wave amplified in the first stage while allowing the space charge wave to propagate into the second stage of the amplifier. In addition, the sever attenuates the reflected wave from the output end of the second stage, and prevents system oscillation due to feedback. The narrow band amplifier serves as the second stage of the system and consists of a ten period iris loaded waveguide. The structure has a 1.2 cm period, and a 1.42 cm external radius. Each iris is 0.6 cm long with an internal radius of 0.62 cm. To couple the power out of the narrow band structure, the width of the last iris is reduced to 0.1 cm. This modification is essential for efficient output coupling. The system is driven by a 950 kV, 1 kA, 50 ns, 0.6 cm diameter electron beam. The output power is determined using far field measurements and has been confirmed calorimetrically.

\* Work supported by USDOE and AFOSR.

As stated earlier substantial electron energy spreads occur during the interaction, with some electrons gaining energy while others lose energy, depending on their phase relative to the wave. The electron energy spread resulting from the amplification process is measured using a small deflection angle magnetic spectrometer. The spectrometer field can be varied to change the energy range of the particles detected by a strip of electron sensitive film. The film is then optically scanned to produce an output electron energy spectrum with the electron deflection calibrated to measure the particle energy.

### III. EXPERIMENTAL RESULTS

The output power of the TWT's is measured using far field measurements of the gain. An independent measurement, up to output levels of 65 MW is obtained from a calorimeter [3].

The output power of the single stage alone is of order 3 MW, and has been increased to 50 MW before *rf* breakdown occurs on the dielectric. The power from the two stage device is measured as a function of input frequency and is shown in fig. 2. Power levels from the calorimetric measurements are also shown to correlate well with the gain data up to 65 MW. Above this level the pressure transducer in the calorimeter saturated. The maximum output power is  $\sim 160$  MW. At these power levels the *rf* pulse duration matched that of the driver electron beam.

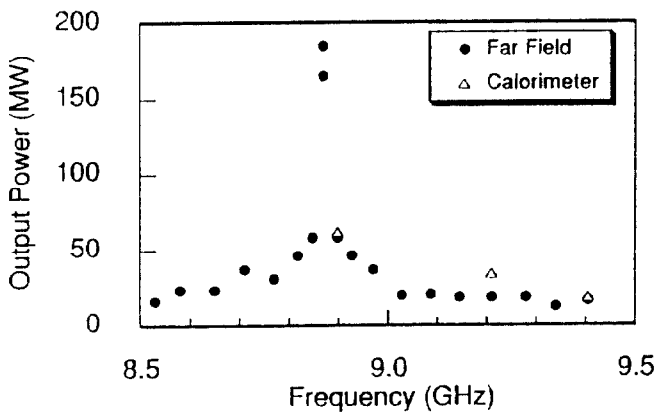


Fig 2. Measured frequency response of the NBS amplifier.

The frequency content of the sampled output signal is measured with a double balanced mixer using heterodyning techniques. A typical fast Fourier transform (FFT) is illustrated in Fig. 3 and is within  $\pm 20$  MHz of the input frequency. Note that the output is single frequency and the sidebands have been eliminated. The electron energy

spectrum is shown in fig. 4 for three sets of conditions.

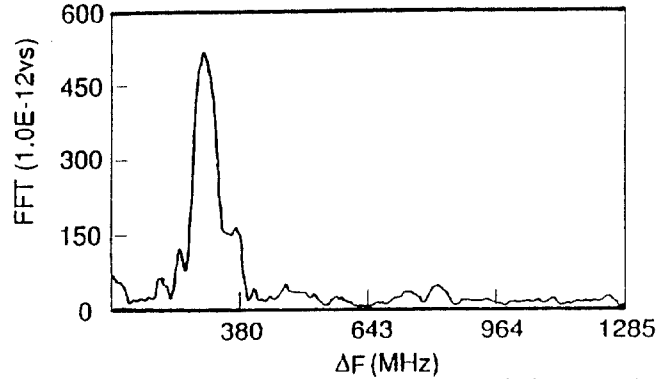


Fig 3. FFT of the measured output signal showing single frequency output.

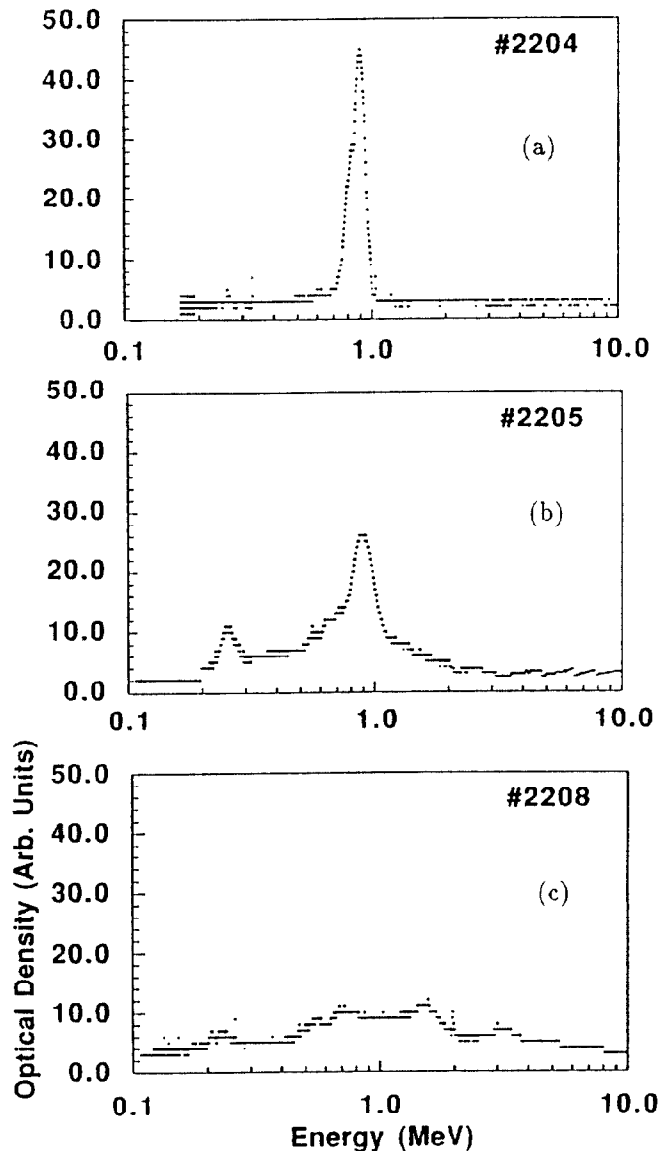


Fig 4. Electron energy spectra at the amplifier output. (a) Injected electron spectrum, (b) output energy spectrum without *rf* input, (c) output energy spectrum with *rf* input.

Fig. 4a shows the spectrum of the injected electron beam. In fig. 4b we show the spectrum without any *rf* input. In this case the wave grows in the amplifier structures from noise, causing a substantial change in the electron momentum distribution. The main peak is at the injection energy of 900 *kV*, but there is also a significant component at 250 *kV*. This component is not present in the absence of the amplifier structures and is clear evidence that the wave growing from noise has extracted energy from the electron beam. The spectrum with *rf* input, fig. 4c, shows a larger spread in electron energies extending from 0.25 – 2 *MV* with a clear component at higher energy than that of the injected beam. In addition the lower energy peak has been smeared out, possibly due to the amplifier being too long and some electrons being reaccelerated.

#### IV. DISCUSSION OF RESULTS

The dispersion relation of the narrow band structure compared to our earlier wide bandwidth (1.7 *GHz*) devices is shown in fig. 5. In the wide pass-band structures an electron velocity spread between 0.8 *c* – 1.0 *c* generates noise in a 300 *MHz* frequency range. In the narrow pass-band (200 *MHz*) structure described here the noise generated is restricted to a range of 20–30 *MHz*. This, in effect, overlaps the input signal and eliminates the sidebands. MAGIC simulations of narrow band amplifiers show single frequency output up to high power levels as shown in fig. 6.

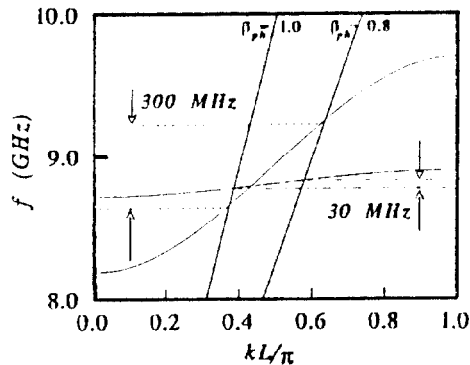


Fig 5. Dispersion relations for a broadband and a narrowband periodic structure.

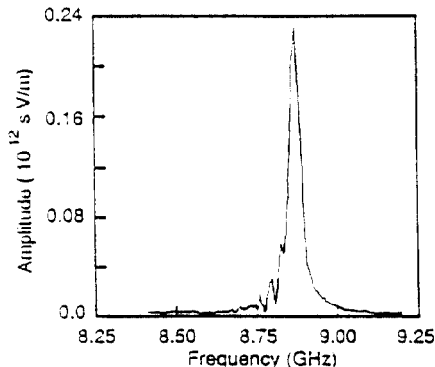


Fig 6. FFT of output signal from narrow band amplifier MAGIC simulation.

The elimination of the sidebands can also be viewed as a transit time isolation. In the 15*cm* long NBS, with a wave energy velocity of  $V_{gr} = 0.007 c$ , it takes about 75 *ns* for a reflected wave to reach the input. This is longer than the electron pulse duration, and consequently the beam is unaffected by the time the reflected wave amplitude becomes significant at the input to the amplifier. At present we are exploring the use of somewhat broader band structures e.g. 400 – 800 *MHz* to identify the limits under which we can operate without sidebands. The shunt impedance of a structure is inversely proportional to the wave group velocity, so the broader band devices will have a lower shunt impedance and hence the electric field of the wave will be lower for a given power flow through the TWT. In addition we are exploring the possibility of interacting with the first space harmonic of a slow wave structure in order to reduce the wave growth rate, and the wave electric field, for a given power flow.

In conclusion, we note that the use of traveling wave tube structures offers an alternate approach for the generation of ultra high power microwave signals. Operation may be in a mode in which a TWT amplifier is used as a stand alone device for microwave generation or as the output structure for a klystron. In the latter scenario the output structure may have additional gain or may be used simply as a device for power extraction. In either case the use of the TWT allows for a reduction in the electric field strength at the output port.

#### V. REFERENCES

- [1] D. Shiffler, J. A. Nation, L. Schächter, J. D. Ivers and G. S. Kerslick, *J. Appl. Phys.*, **70**, 106, (1991).
- [2] L. Schächter, J. A. Nation and D. Shiffler, *J. Appl. Phys.*, **70**, 114, (1991).
- [3] C. B. Wharton, L. M. Earley, and W. P. Ballard, *Rev. Sci. Instrum.*, **57**, 855 (1986).